

Molecular Dynamics Simulation of the Specific Heat of Undercooled Fe-Ni Melts¹

C. Yang,² M. Chen,^{2,3} and Z. Y. Guo²

In this paper, a molecular dynamics simulation based on the embedded-atom method (EAM) is applied to calculate the specific heat capacity of the Fe-33% Ni alloy at temperatures above and below the melting temperature. The relationship between the specific heat of the alloy and undercooling is investigated. The heat capacity of the Fe-Ni alloy is a constant in the superheated and undercooled liquid states. Comparisons between previous work and the current study show that the heat capacity behavior of undercooled alloy strongly depends on the species of the alloy.

KEY WORDS: embedded-atom method; Fe-Ni alloy; heat capacity; molecular dynamics simulation; undercooled liquid melt.

1. INTRODUCTION

A knowledge of the thermodynamic properties of the undercooled liquid is necessary to characterize this metastable state and to describe the solidification behavior of undercooled melts. In particular, specific heats are of interest because knowledge of the specific heat of the undercooled liquid can give some information about the speed of crystal growth [1], short-range order of liquids [2], nucleation rate [3] and the ideal glass transition temperature [4]. However, there are few experimental data for the specific heat capacities of undercooled melts, especially for high-melting-point metals. This is because it is difficult to avoid the crystallization of undercooled melts on a time scale that allows for calorimetric investigations. As a result, the demand for reliable predictive methods continues.

¹ Paper presented at the Fourteenth Symposium on Thermophysical Properties, June 25–30, 2000, Boulder, Colorado, U.S.A.

² Department of Engineering Mechanics, Tsinghua University, Beijing 100084, China.

³ To whom correspondence should be addressed. E-mail: mchen@tsinghua.edu.cn

Molecular dynamics simulation (MDS) is a powerful method developed over the past decades, which has been widely used in materials science. With the development of high performance computers, atomic-scale simulations have proven to be an effective method for understanding preparation processes for materials and predicting thermophysical properties in some extreme cases. Fe-Ni alloys are widely used as a corrosion-resistant material. However, there is a lack of experimental heat capacity data for Fe-Ni alloys, especially in the undercooled region. The main purpose of this paper is to predict the specific heat of the Fe-33% Ni alloy by MDS.

2. EMBEDDED-ATOM METHOD

The embedded-atom method (EAM) has achieved significant success in describing the interaction of atoms of metals and alloys. It has been shown to give good results in simulations of thermal expansion, surface and liquid structure, and even the undercooled liquid-to-glass and liquid-to-crystalline transitions.

The EAM is a procedure for designing a mathematical model of a metal, which was originally developed by researchers at Sandia National Laboratory [5, 6]. The basic equations of the EAM are [6]

$$E_{\text{tot}} = \sum_i F_i(\rho_i) + \frac{1}{2} \sum_{i,j (i \neq j)} \phi_{i,j}(R_{i,j}) \quad (1)$$

$$\rho_i = \sum_{i \neq j} f_j(R_{i,j}) \quad (2)$$

where E_{tot} is the total internal energy, ρ_i is the electron density at atom i due to all other atoms, f_j is the electron density of atom j as a function of distance from its center, $R_{i,j}$ is the separation distance between atoms i and j , $F_i(\rho_i)$ is the energy to embed atom i in an electron density ρ_i , and $\phi_{i,j}$ is the two-body central potential between atoms i and j . In this paper, the analytic nearest-neighbor model developed by Johnson [7, 8] was adopted. Following Johnson, the embedded energy for iron is [7]

$$F(\rho) = -(E_c - E_{1f}) \left(1 - \gamma \ln \left(\frac{\rho}{\rho_e} \right) \right) \left(\frac{\rho}{\rho_e} \right)^\gamma \quad (3)$$

$$f(r) = f_e (r_{1e}/r)^\beta \quad (4)$$

and for nickel is [8]

$$F(\rho) = -E_c \left[1 - \gamma \ln \left(\frac{\rho}{\rho_e} \right) \right] \left[\frac{\rho}{\rho_e} \right]^\gamma - \Phi_e \left[\frac{\rho}{\rho_e} \right]^\gamma \quad (5)$$

For iron, the monatomic pair potential is as follows [7]:

$$\phi(r) = k_3 \left(\frac{r}{r_{1e}} - 1 \right)^3 + k_2 \left(\frac{r}{r_{1e}} - 1 \right)^2 + k_1 \left(\frac{r}{r_{1e}} - 1 \right) + k_0 \quad (5)$$

For nickel, the monatomic pair potential is as follows [8]:

$$\phi(r) = \phi_e \exp \left(\gamma \left(\frac{r}{r_{1e}} - 1 \right) \right) \quad (6)$$

Since the electron density at any location is taken as a linear superposition of atomic electron densities, and the embedding energy is assumed to be independent of the source of the electron density, the electron density functions can be taken directly from monatomic models. For two different types of atoms (*a*-type and *b*-type), the pair interaction is modeled as [8]

$$\phi^{ab}(r) = \frac{1}{2} \left(\frac{f^b(r)}{f^a(r)} \phi^{aa}(r) + \frac{f^a(r)}{f^b(r)} \phi^{bb}(r) \right) \quad (7)$$

The superscripts *a* and *b* indicate the *a*- and *b*-type atoms in a binary alloy. $\phi^{aa}(r)$ and $\phi^{bb}(r)$ are the monatomic potentials which can be determined from monatomic models.

3. SIMULATION DETAILS

Usually, there are two kinds of statistical methods utilized in calculating the specific heat. The first is to derive the specific heat from the fluctuation of energy [9]

$$C_v = \frac{\langle \delta E^2 \rangle_{NVT}}{K_B T^2} \quad (8)$$

The second is to determine the specific heat from the differential of the energy function of temperature

$$C_v = \frac{dE(T)}{dT} \quad (9)$$

Considering the capabilities of the computer system, 500 molecules were simulated. Since there are only 500 molecules in our simulation system, the calculation of C_v via the fluctuation of energy method is not stable. So, in this paper, the second method is adopted.

Table I. Input Parameters and Model Parameters for Nickel [8]

E_{1f} (eV)	E_c (eV)	f_e	ϕ_e (eV)	β	γ
1.6	4.45	0.41	0.74	6.41	8.86

At the beginning of the simulation, 334 iron and 166 nickel atoms were arranged in a face-centered cubic box subject to periodic boundary conditions. The time step was 5.0×10^{-15} s. In order to get an equilibrium liquid state in the simulation, the system started at 2100 K which is above the melting point. This temperature was kept constant for 500,000 steps. Then the quenching process with a cooling rate of $4 \times 10^{11} \text{ K} \cdot \text{s}^{-1}$ was carried out to calculate the internal energy E at 100 K intervals of temperature. At each temperature, 400,000 steps were carried out for relaxation. Then 100,000 more steps were taken to calculate the internal energy E . The simulation was stopped at 1200 K, which is 533 K lower than the melting point. Since the quenching process is very fast, the alloy stays in the undercooled liquid state. All the parameters used in the simulation are shown in Tables I and II.

The simulation results for the internal energy E are shown in Fig. 1. The energy has a linear relationship with temperature. This implies that the constant-volume heat capacity is a constant $457 \text{ J} \cdot \text{kg}^{-1} \cdot \text{K}^{-1}$ in the region between 1200 and 2100 K, as shown in Fig. 2. To compare with experimental results, the calculated constant-volume heat capacities have been transformed into constant-pressure values. For nickel, the calculated C_p is $39.2 \text{ J} \cdot \text{mol}^{-1} \cdot \text{K}^{-1}$ while the measured values are $43.09 \text{ J} \cdot \text{mol}^{-1} \cdot \text{K}^{-1}$ [11] and $41 \pm 1 \text{ J} \cdot \text{mol}^{-1} \cdot \text{K}^{-1}$ [12]. The deviations are within 9 percent. For iron, the calculated C_p is $44.8 \text{ J} \cdot \text{mol}^{-1} \cdot \text{K}^{-1}$ while the measured values are $46.02 \text{ J} \cdot \text{mol}^{-1} \cdot \text{K}^{-1}$ [11] and $47 \pm 1 \text{ J} \cdot \text{mol}^{-1} \cdot \text{K}^{-1}$ [12]. The deviations are within 7 percent. The calculated heat capacity of Fe-33% Ni alloy is not compared with experimental results because no experimental data for this alloy in the undercooled region are available. The heat capacity of Fe-33% Ni alloy behaves differently as compared with the heat capacities of Cu-Ni alloys [13]. The simulation results of heat capacity of Cu-25% Ni alloy exhibit a slight decrease with increasing temperature in the region from

Table II. Input Parameters and Model Parameters for Iron, k_i ($i=0, 1, 2, 3$) in $\text{eV} \cdot \text{\AA}^{-1}$ [10]

E_c (eV)	E_{1f} (eV)	γ	f_e	k_3	k_2	k_1	k_0
4.29	1.79	0.37	0.36	-13.31	9.21	-0.88	-0.27

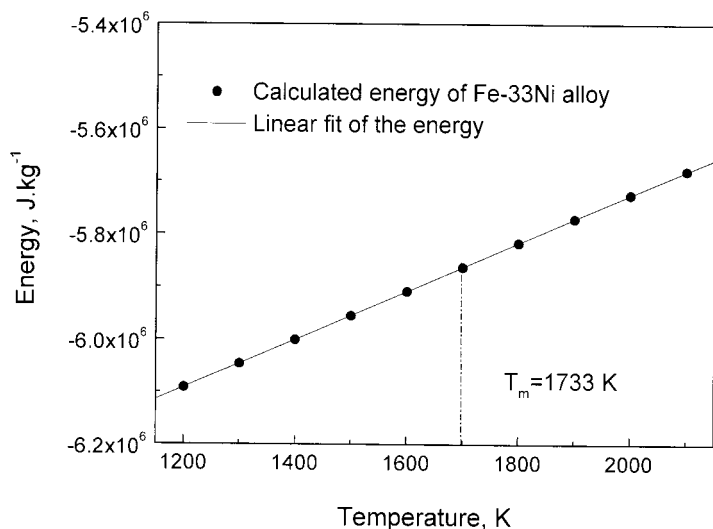


Fig. 1. Local-average internal energy of Fe-33% Ni.

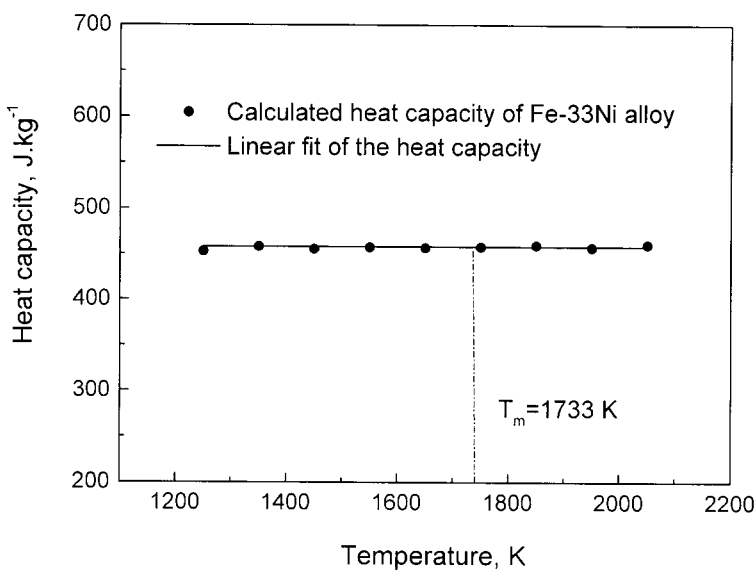


Fig. 2. Simulation results of heat capacity of Fe-33% Ni.

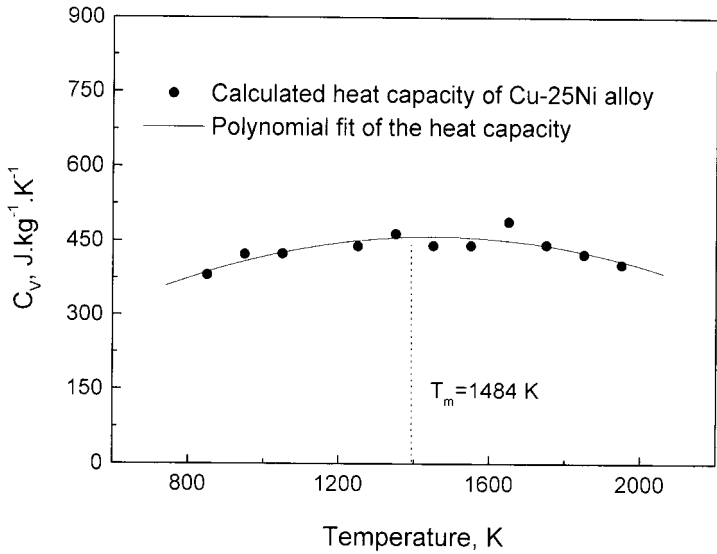


Fig. 3. Simulation results of heat capacity of Cu-25% Ni.

1100 to 2000 K, while C_v increases with temperature in the region from 800 to 1100 K (shown as Fig. 3). Experimental measurements of some undercooled liquid metals and alloys revealed that the heat capacities could be remarkably different from those of liquid states above the melting point [14]. Whereas, the other measurements of several pure liquid metals indicated that no apparent change of heat capacities could be expected in the undercooled region [11, 12]. In molecular dynamics simulations, the heat capacities of Cu-Ni alloys indicated pronounced dependence on undercoolings [13], while those of the Fe-Ni alloy exhibit here a constant value. The behavior of the heat capacities in the undercooled region might depend on the species of the alloys.

4. CONCLUSIONS

The specific heat of Fe-33% Ni alloy was simulated with a molecular dynamics simulation based on EAM. The simulation was performed at conditions ranging from the undercooled to superheated regions. The results show that the heat capacity of liquid Fe-33% Ni above and below the melting point exhibits a constant value. Thus, in the prediction of crystal growth and the nucleation rate, an average heat capacity is suitable. The simulation results of pure liquid nickel and iron in the undercooled region are in reasonable agreement with experimental data. However, the

calculated heat capacity of Fe-33% Ni alloy is not compared with experimental results because experimental data for this alloy in the undercooled region are not available. Molecular dynamics simulations show that the behavior of the heat capacity of the alloys in the undercooled region might strongly depend on the constituents.

ACKNOWLEDGMENTS

This research is supported by the National Natural Science Foundation of China under Grant No. 59876016, the Project of High Technology & Development Program of China (863 program), the Fundamental Research Foundation, the Tongfang High Performance Computation Foundation, and the Doctoral Education Foundation of Tsinghua University.

REFERENCES

1. G. P. Ivantsov, *Dokl. Akad. Nauk. SSSR* **58**:567 (1947).
2. D. R. Nelson, M. Rubinstein, and F. Spaepen, *Phil. Mag.* **A46**:105 (1982).
3. B. Wei, N. Wang, M. Barth, and D. M. Herlach, *Acta Metallurgica Sinica/Jinshu Xuebao* **30**:B290 (1994).
4. W. Kauzmann, *Chem. Rev.* **43**:219 (1948).
5. M. S. Daw and M. I. Baskes, *Phys. Rev. Lett.* **50**:1285 (1983).
6. M. S. Daw and M. I. Baskes, *Phys. Rev.* **B29**:6443 (1984).
7. R. A. Johnson and D. J. Oh, *J. Mat. Res.* **4**:1195 (1989).
8. R. A. Johnson, *Phys. Rev.* **B39**:12554 (1989).
9. M. P. Allen and D. J. Tildesley, *Computer Simulation of Liquids* (Clarendon Press, Oxford, 1989).
10. B. W. Zhang and Y. F. Ouyang, *Phys. Rev.* **B48**:3022 (1993).
11. K. Schaefer, M. Rosner-Kuhn, and M. G. Froberg, *Mat. Sci. Eng.* **A197**:83 (1995).
12. M. Barth, F. Joo, B. Wei, and D. M. Herlach, *J. Non-Crystalline Solid* **156-158**:398 (1993).
13. C. Yang, *Molecular Dynamics Simulation and Experimental Investigation on Heat Capacities of Liquid Metals*, Ph.D. dissertation (Tsinghua University, P.R. China, 2000).
14. S. G. Klose, P. S. Frankwicz, and H.-J. Fecht, *Mat. Sci Forum* **179-181**:729 (1995).